ISSN 0965-5425, Computational Mathematics and Mathematical Physics, 2021, Vol. 61, No. 9, pp. 1432–1443. © Pleiades Publishing, Ltd., 2021.

PARTIAL DIFFERENTIAL EQUATIONS

Optical Solitons for Chen–Lee–Liu Equation with Two Spectral Collocation Approaches

M. A. Abdelkawy[a,b,*], S. S. Ezz-Eldien[c,d], A. Biswas[e,f,g,h], A. Kamis Alzahrani[f], and M. R. Belic[i]

[a] *Department of Mathematics and Statistics, College of Science, Imam Mohammad Ibn Saud Islamic University, Riyadh, Saudi Arabia*

[b] *Department of Mathematics, Faculty of Science, Beni-Suef University, Beni-Suef, Egypt*

[c] *Nanjing Normal Univ., Sch. Math. Sci., Jiangsu Key Lab NSLSCS, Nanjing, Jiangsu, 210023 China*

[d] *New Valley Univ., Dept Math, Fac. Sci., Kharga, 72511 Egypt*

[e] *Department of Physics, Chemistry and Mathematics, Alabama A&M University, Normal, AL, 35762-4900 USA*

[f] *Mathematical Modeling and Applied Computation (MMAC) Research Group, Department of Mathematics, King Abdulaziz University, Jeddah, 21589 Saudi Arabia*

[g] *Department of Applied Mathematics, National Research Nuclear University, Moscow, 115409 Russia*

[h] *Department of Mathematics and Applied Mathematics, Sefako Makgatho Health Sciences University, Medunsa, Pretoria, 0204 South Africa*

[i] *Institute of Physics Belgrade, Pregrevica 118, 11080 Zemun, Serbia*

**e-mail: melkawy@yahoo.com*

Received May 12, 2020; revised May 12, 2020; accepted May 20, 2021

Abstract—This paper revisits the study of optical solitons that is governed by one of the three forms of derivative nonlinear Schrödinger's equation that is also known as Chen–Lee–Liu model. This model is investigated by the aid of fully shifted Jacobi's collocation method with two independent approaches. The first is discretization of the spatial variable, while the other is discretization of the temporal variable. It is concluded that the method of the current paper is far more efficient and reliable for the considered model. Numerical results illustrate the performance efficiency of the algorithm. The results also point out that the scheme can lead to spectral accuracy of the studied model.

Keywords: Chen–Lee–Liu equation, collocation method, shifted Jacobi–Gauss–Lobatto quadrature, shifted Jacobi–Gauss–Radau quadrature

DOI: 10.1134/S0965542521090025

1. INTRODUCTION

The theory of optical solitons [1–5] is mainly governed by the well-known nonlinear Schrödinger's equation (NLSE) [6–9]. However, there exists a wide variety of its manifestations and modifications that also govern pulse transfer across the globe through optical fibers, PCF, metamaterials and couplers. A few such models are Schrödinger–Hirota equation [10], Manakov equation, complex Ginzburg–Landau equation, Fokas–Lennels equation, Gabitov–Turitsyn equation and many others. These models are considered under different circumstances such as dispersive solitons, differential group delay, DM solitons and many others. Besides these familiar models, there is another class of versions of NLSE that is referred to as derivative NLSE (DNLSE) [11–13] that appears in three forms. One such form is the Chen–Lee–Liu equation [14–21] that incorporates higher order perturbations from optics and is going to be the focus of today's paper. While a plethora of pre-existing work has been already reported in regards to this model, today's focus is going to be handling the model by the aid of fully shifted Jacobi's collocation method.

Several numerical methods, including local and global methods, have been listed as approximate techniques for treating the differential equations. The local methods listed the approximate solution at specific points, while the global methods give the approximate solution in whole the mentioned interval. The numerical approximations for differential equations [22–26] are listed at specific points using finite difference methods. While the finite element methods subdivides the whole interval into sub-intervals and give the approximate solution in they. The finite element methods are used for various types of differential equation, see, for example, [27–30].

Recently, there are more interest of appointing the spectral methods to treat with various kinds of differential and integral equations [31–33], due to their applicability to bounded and unbounded domains [34–37]. The convergence speed is one of the major advantages of spectral method. Spectral methods have exponential convergence rates as will as a high accuracy level. The spectral method has been classified to four classes, collocation [39], tau [40], Galerkin [41] and Petrov–Galerkin [42] method.

Shifted Jacobi collocation scheme is used to numerically solve the Chen–Lee–Liu equation [43–47] with initial-boundary and initial-non-local conditions. The solution $\mathscr{Z}(x,t)$ is firstly placed in its real $\mathscr{U}(x,t)$ and imaginary $\mathscr{V}(x,t)$ parts. Accordingly, the real $\mathscr{U}(x,t)$ and imaginary $\mathscr{V}(x,t)$ parts of such equation is approximated as $\mathscr{U}_{\mathscr{N},\mathscr{M}}(x,t)$ and $\mathscr{V}_{\mathscr{N},\mathscr{M}}(x,t)$, respectively, which can be expressed as a finite expansion of shifted Jacobi polynomials for spatial variable. Subsequently, the Chen–Lee–Liu equation with boundary or non-local conditions is reduced to temporal differential system with initial conditions. Then, the Shifted Jacobi–Gauss–Radau collocation is assigned for temporal discretization, which is more reliable for treating with such problems. Substituting these discretizations in the mentioned equation gets a nonlinear system of algebraic equations which solved numerically using Newton–Raphson approach.

The mentioned scheme is implemented for the Chen–Lee–Liu equation with initial-boundary and initial-non-local conditions in Section 2. The competence of our numerical approach is exhibited by diverse examples in Section 3. Few remarks are mentioned in the last section.

2. CHEN–LEE–LIU EQUATION

Here, we treat with the Chen–Lee–Liu equation with initial-boundary and initial-non-local conditions.

2.1. Initial-Boundary Conditions

We consider the Chen–Lee–Liu equation

$$i\frac{\partial\mathscr{Z}(x,t)}{\partial t}+\frac{\partial^2\mathscr{Z}(x,t)}{\partial x^2}+i\gamma\left|\mathscr{Z}(x,t)\right|^2\frac{\partial\mathscr{Z}(x,t)}{\partial x}=0,\quad (x,t)\in[0,\mathscr{L}]\times[0,T], \tag{2.1}$$

with

$$\begin{gathered}\mathscr{Z}(0,t)=\chi_1(t),\quad \mathscr{Z}(\mathscr{L},t)=\chi_2(t),\quad t\in[0,T],\\ \mathscr{Z}(x,0)=\xi_1(x),\quad x\in[0,\mathscr{L}].\end{gathered} \tag{2.2}$$

Letting the complex functions ($\mathscr{Z}(x,t)$, $\chi_1(t)$, $\chi_2(t)$, and $\xi_1(x)$) to be in their real and imaginary parts as:

$$\begin{gathered}\mathscr{Z}(x,t)=\mathscr{U}(x,t)+i\mathscr{V}(x,t),\quad \chi_1(t)=\eta_1(t)+i\eta_3(t),\\ \chi_2(t)=\eta_2(t)+i\eta_4(t),\quad \phi_1(t)=\varphi_1(x)+i\varphi_2(x),\end{gathered} \tag{2.3}$$

wheresoever $\mathscr{U}(x,t)$, $\mathscr{V}(x,t)$, $f(x,t)$, $g(x,t)$, $\eta_1(t)$, $\eta_3(t)$, $\eta_2(t)$, $\eta_4(t)$, $\varphi_1(x)$ and $\varphi_2(x)$, are real functions, thereafter

$$\begin{gathered}\frac{\partial\mathscr{U}(x,t)}{\partial t}+\frac{\partial^2\mathscr{V}(x,t)}{\partial x^2}+\gamma(u^2(x,t)+v^2(x,t))\frac{\partial\mathscr{U}(x,t)}{\partial x}=0,\\ \frac{\partial\mathscr{V}(x,t)}{\partial t}-\frac{\partial^2\mathscr{U}(x,t)}{\partial x^2}+\gamma(u^2(x,t)+v^2(x,t))\frac{\partial\mathscr{V}(x,t)}{\partial x}=0,\end{gathered} \tag{2.4}$$

with the next conditions

$$\begin{gathered}\mathscr{U}(0,t)=\eta_1(t),\quad \mathscr{U}(\mathscr{L},t)=\eta_2(t),\quad t\in[0,T],\\ \mathscr{V}(0,t)=\eta_3(t),\quad \mathscr{V}(\mathscr{L},t)=\eta_4(t),\quad t\in[0,T],\\ \mathscr{U}(x,0)=f_1(x),\quad \mathscr{V}(x,0)=f_2(x),\quad x\in[0,\mathscr{L}].\end{gathered} \tag{2.5}$$

The distributed of shifted Jacobi–Gauss–Lobatto quadrature points in $[0,\mathscr{L}]$ is the major merit of utilizing them. Here, we list the basic step of implementing shifted Jacobi–Gauss–Lobatto collocation method

for transforming the nonlinear system (2.4), (2.5) to temporal differential system with initial conditions. $\mathcal{U}(x,t)$ and $\mathcal{V}(x,t)$ are approximated as

$$\mathcal{U}_{\mathcal{N}}(x,t)=\sum_{j=0}^{\mathcal{N}}\epsilon_j(t)\mathcal{P}_{\mathcal{L},j}^{(\alpha_1,\beta_1)}(x),\qquad \mathcal{V}_{\mathcal{N}}(x,t)=\sum_{j=0}^{\mathcal{N}}\varepsilon_j(t)\mathcal{P}_{\mathcal{L},j}^{(\alpha_1,\beta_1)}(x), \tag{2.6}$$

the orthogonal property and discrete inner product [6] permit the following

$$\begin{aligned}\epsilon_j(t)&=\frac{1}{h_{\mathcal{L},k}^{(\alpha_1,\beta_1)}}\sum_{i=0}^{N}P_j(x_{\mathcal{L},\mathcal{N},i}^{(\alpha_1,\beta_1)})\varpi_{\mathcal{L},\mathcal{N},i}^{(\alpha_1,\beta_1)}\mathcal{U}(x_{\mathcal{L},\mathcal{N},i}^{(\alpha_1,\beta_1)},t),\\ \varepsilon_j(t)&=\frac{1}{h_{\mathcal{L},k}^{(\alpha_1,\beta_1)}}\sum_{i=0}^{N}P_j(x_{\mathcal{L},\mathcal{N},i}^{(\alpha_1,\beta_1)})\varpi_{\mathcal{L},\mathcal{N},i}^{(\alpha_1,\beta_1)}\mathcal{V}(x_{\mathcal{L},\mathcal{N},i}^{(\alpha_1,\beta_1)},t).\end{aligned} \tag{2.7}$$

In that case, Eq. (2.6) take the form

$$\begin{aligned}\mathcal{U}(x,t)&=\sum_{i=0}^{\mathcal{N}}\left(\sum_{j=0}^{\mathcal{N}}\frac{1}{h_{\mathcal{L},k}^{(\alpha_1,\beta_1)}}\mathcal{P}_{\mathcal{L},j}^{(\alpha_1,\beta_1)}(x_{\mathcal{L},\mathcal{N},i}^{(\alpha_1,\beta_1)})\mathcal{P}_{\mathcal{L},j}^{(\alpha_1,\beta_1)}(x)\varpi_{\mathcal{L},\mathcal{N},i}^{(\alpha_1,\beta_1)}\right)\mathcal{U}(x_{\mathcal{L},\mathcal{N},i}^{(\alpha_1,\beta_1)},t),\\ \mathcal{V}(x,t)&=\sum_{i=0}^{\mathcal{N}}\left(\sum_{j=0}^{\mathcal{N}}\frac{1}{h_{\mathcal{L},k}^{(\alpha_1,\beta_1)}}\mathcal{P}_{\mathcal{L},j}^{(\alpha_1,\beta_1)}(x_{\mathcal{L},\mathcal{N},i}^{(\alpha_1,\beta_1)})\mathcal{P}_{\mathcal{L},j}^{(\alpha_1,\beta_1)}(x)\varpi_{\mathcal{L},\mathcal{N},i}^{(\alpha_1,\beta_1)}\right)\mathcal{V}(x_{\mathcal{L},\mathcal{N},i}^{(\alpha_1,\beta_1)},t).\end{aligned} \tag{2.8}$$

Over and above that, the partial derivative of first order in space evaluated at shifted Jacobi–Gauss–Lobatto collocation as

$$\begin{aligned}\frac{\partial\mathcal{U}(x_{\mathcal{L},\mathcal{N},n}^{(\alpha_1,\beta_1)},t)}{\partial x}&=\sum_{i=0}^{\mathcal{N}}\rho_{n,i}\mathcal{U}(x_{\mathcal{L},\mathcal{N},i}^{(\alpha_1,\beta_1)},t),\\ \frac{\partial\mathcal{V}(x_{\mathcal{L},\mathcal{N},n}^{(\alpha_1,\beta_1)},t)}{\partial x}&=\sum_{i=0}^{\mathcal{N}}\rho_{n,i}\mathcal{V}(x_{\mathcal{L},\mathcal{N},i}^{(\alpha_1,\beta_1)},t),\qquad n=0,1,\ldots,N,\end{aligned} \tag{2.9}$$

where

$$\rho_{n,i}=\sum_{j=0}^{\mathcal{N}}\frac{\varpi_{\mathcal{L},\mathcal{N},i}^{(\alpha_1,\beta_1)}}{h_{\mathcal{L},k}^{(\alpha_1,\beta_1)}}\mathcal{P}_{\mathcal{L},j}^{(\alpha_1,\beta_1)}(x_{\mathcal{L},\mathcal{N},i}^{(\alpha_1,\beta_1)})\left(\frac{\partial\mathcal{P}_{\mathcal{L},j}^{(\alpha_1,\beta_1)}(x)}{\partial x}\right)\Bigg|_{x=x_{\mathcal{L},\mathcal{N},n}^{(\alpha_1,\beta_1)}}. \tag{2.10}$$

Comparable procedure can be performed to the partial derivative of order two for space variable to get

$$\begin{aligned}\frac{\partial^2\mathcal{U}(x_{\mathcal{L},\mathcal{N},n}^{(\alpha_1,\beta_1)},t)}{\partial x^2}&=\sum_{i=0}^{\mathcal{N}}\lambda_{n,i}\mathcal{U}(x_{\mathcal{L},\mathcal{N},i}^{(\alpha_1,\beta_1)},t),\\ \frac{\partial^2\mathcal{V}(x_{\mathcal{L},\mathcal{N},n}^{(\alpha_1,\beta_1)},t)}{\partial x^2}&=\sum_{i=0}^{\mathcal{N}}\lambda_{n,i}\mathcal{V}(x_{\mathcal{L},\mathcal{N},i}^{(\alpha_1,\beta_1)},t),\qquad n=0,1,\ldots,N,\end{aligned} \tag{2.11}$$

where

$$\lambda_{n,i}=\sum_{j=0}^{\mathcal{N}}\frac{\varpi_{\mathcal{L},\mathcal{N},i}^{(\alpha_1,\beta_1)}}{h_{\mathcal{L},k}^{(\alpha_1,\beta_1)}}\mathcal{P}_{\mathcal{L},j}^{(\alpha_1,\beta_1)}(x_{\mathcal{L},\mathcal{N},i}^{(\alpha_1,\beta_1)})\left(\frac{\partial^2\mathcal{P}_{\mathcal{L},j}^{(\alpha_1,\beta_1)}(x)}{\partial x^2}\right)\Bigg|_{x=x_{\mathcal{L},\mathcal{N},n}^{(\alpha_1,\beta_1)}}. \tag{2.12}$$

Combining the boundary conditions with the above-mentioned equations and equalizing the residual of (2.1) by zero give us

$$\begin{aligned}\dot{\mathcal{U}}_n(t)&=-\lambda_{n,0}\eta_3(t)-\lambda_{n,\mathcal{N}}\eta_4(t)-\sum_{i=1}^{\mathcal{N}-1}\lambda_{n,i}\mathcal{V}_i(t)-\gamma(\mathcal{U}_n^2(t)+\mathcal{V}_n^2(t))\left(\rho_{n,0}\eta_1(t)+\rho_{n,\mathcal{N}}\eta_2(t)+\sum_{i=1}^{\mathcal{N}-1}\rho_{n,i}\mathcal{U}_i(t)\right),\\ \dot{\mathcal{V}}_n(t)&=\lambda_{n,0}\eta_1(t)+\lambda_{n,\mathcal{N}}\eta_2(t)+\sum_{i=1}^{\mathcal{N}-1}\lambda_{n,i}\mathcal{U}_i(t)-\gamma(\mathcal{U}_n^2(t)+\mathcal{V}_n^2(t))\left(\rho_{n,0}\eta_3(t)+\rho_{n,\mathcal{N}}\eta_3(t)+\sum_{i=1}^{\mathcal{N}-1}\rho_{n,i}\mathcal{V}_i(t)\right),\\ &n=1,2,\ldots,\mathcal{N}-1,\end{aligned} \tag{2.13}$$

with initial values

$$\mathcal{U}_n(0) = f_1(x^{(\alpha_1,\beta_1)}_{\mathcal{L},\mathcal{N},n}), \quad \mathcal{V}_n(0) = f_2(x^{(\alpha_1,\beta_1)}_{\mathcal{L},\mathcal{N},n}), \quad n = 1,\ldots,\mathcal{N}-1, \tag{2.14}$$

where

$$\mathcal{U}_k(t) = \mathcal{U}(x^{(\alpha_1,\beta_1)}_{\mathcal{L},\mathcal{N},k}, t), \quad \mathcal{V}_k(t) = \mathcal{V}(x^{(\alpha_1,\beta_1)}_{\mathcal{L},\mathcal{N},k}, t), \quad k = 1,\ldots,N-1.$$

The numerical approach of the such system will listed in Subsection 2.3.

2.2. Non-Local Condition

The nonlocal conditions will treat in this subsection. Let us consider

$$i\frac{\partial \mathcal{Z}(x,t)}{\partial t} + \frac{\partial^2 \mathcal{Z}(x,t)}{\partial x^2} + i\gamma\left|\mathcal{Z}(x,t)\right|^2 \mathcal{Z}(x,t) = 0, \quad (x,t) \in [0,\mathcal{L}]\times[0,T], \tag{2.15}$$

with the initial, boundary and non-local conditions

$$\begin{gathered}\mathcal{Z}(0,t) = \chi_1(t), \quad \int_{\iota_1}^{\iota_2} \mathcal{Z}(x,t)dx = \chi_2(t), \quad 0 \le \iota_1 < \iota_2 \le \mathcal{L}, \quad t \in [0,T], \\ \mathcal{Z}(x,0) = \phi_1(x), \quad x \in [0,\mathcal{L}].\end{gathered} \tag{2.16}$$

Using comparable analysis in Subsection 2.1, we get

$$\begin{aligned}&\frac{\partial \mathcal{U}(x,t)}{\partial t} + \frac{\partial^2 \mathcal{V}(x,t)}{\partial x^2} + \gamma(u^2(x,t)+v^2(x,t))\frac{\partial \mathcal{U}(x,t)}{\partial x} = 0, \\ &\frac{\partial \mathcal{V}(x,t)}{\partial t} - \frac{\partial^2 \mathcal{U}(x,t)}{\partial x^2} + \gamma(u^2(x,t)+v^2(x,t))\frac{\partial \mathcal{V}(x,t)}{\partial x} = 0,\end{aligned} \tag{2.17}$$

with the initial, boundary and non-local conditions

$$\begin{gathered}\mathcal{U}(0,t) = \eta_1(t), \quad \int_{\iota_1}^{\iota_2} \mathcal{U}(x,t)dx = \eta_2(t), \quad 0 \le \iota_1 < \iota_2 \le \mathcal{L}, \quad t \in [0,T], \\ \mathcal{V}(0,t) = \eta_3(t), \quad \int_{\iota_1}^{\iota_2} \mathcal{V}(x,t)dx = \eta_4(t), \quad 0 \le \iota_1 < \iota_2 \le \mathcal{L}, \quad t \in [0,T], \\ \mathcal{U}(x,0) = f_1(x), \quad \mathcal{V}(x,0) = f_2(x), \quad x \in [0,\mathcal{L}].\end{gathered} \tag{2.18}$$

The integral conditions in (2.18) are treated as

$$\int_{\iota_1}^{\iota_2} \sum_{i=0}^{\mathcal{N}} \left(\sum_{j=0}^{\mathcal{N}} \frac{1}{h^{(\alpha_1,\beta_1)}_{\mathcal{L},j}} \mathcal{P}^{(\alpha_1,\beta_1)}_{\mathcal{L},j}(x^{(\alpha_1,\beta_1)}_{\mathcal{L},\mathcal{N},n}) \mathcal{P}^{(\alpha_1,\beta_1)}_{\mathcal{L},j}(x) \varpi^{(\alpha_1,\beta_1)}_{\mathcal{L},\mathcal{N},i} \right) \mathcal{U}_i(t)dx = \eta_2(t), \quad 0 \le \iota_1 < \iota_2 \le \mathcal{L}, \tag{2.19}$$

which equivalent

$$\sum_{i=0}^{\mathcal{N}} \left(\sum_{j=0}^{\mathcal{N}} \frac{1}{h^{(\alpha_1,\beta_1)}_{\mathcal{L},j}} \mathcal{P}^{(\alpha_1,\beta_1)}_{\mathcal{L},j}(x^{(\alpha_1,\beta_1)}_{\mathcal{L},\mathcal{N},n}) \left(\int_{\iota_1}^{\iota_2} \mathcal{P}^{(\alpha_1,\beta_1)}_{\mathcal{L},j}(x)dx \right) \varpi^{(\alpha_1,\beta_1)}_{\mathcal{L},\mathcal{N},i} \right) \mathcal{U}_i(t) = \eta_2(t), \quad 0 \le a_1 < a_2 \le L, \tag{2.20}$$

or briefly

$$\sum_{i=0}^{\mathcal{N}} I_i \mathcal{U}_i(t) = \eta_2(t), \quad 0 \le \iota_1 < \iota_2 \le \mathcal{L}, \tag{2.21}$$

where

$$I_i = \sum_{j=0}^{\mathcal{N}} \frac{1}{h^{(\alpha_1,\beta_1)}_{\mathcal{L},j}} \mathcal{P}^{(\alpha_1,\beta_1)}_{\mathcal{L},j}(x^{(\alpha_1,\beta_1)}_{\mathcal{L},\mathcal{N},n}) \left(\int_{\iota_1}^{\iota_2} \mathcal{P}^{(\alpha_1,\beta_1)}_{\mathcal{L},j}(x)dx \right) \varpi^{(\alpha_1,\beta_1)}_{\mathcal{L},\mathcal{N},i},$$

similarly, we get

$$\sum_{i=0}^{\mathcal{N}} I_i \mathcal{V}_i(t) = \eta_4(t), \quad 0 \le \iota_1 < \iota_2 \le \mathcal{L}, \tag{2.22}$$

so, yields

$$\begin{aligned}
\mathcal{U}_{\mathcal{N}}(t) &= \frac{1}{I_{\mathcal{N}}}\left(\eta_2(t) - I_0\mathcal{U}_0(t) - \sum_{i=1}^{\mathcal{N}-1} I_i\mathcal{U}_i(t)\right) = \frac{1}{I_{\mathcal{N}}}\left(\eta_2(t) - I_0\eta_1(t) - \sum_{i=1}^{\mathcal{N}-1} I_i\mathcal{U}_i(t)\right),\\
\mathcal{V}_{\mathcal{N}}(t) &= \frac{1}{I_{\mathcal{N}}}\left(\eta_4(t) - I_0\mathcal{V}_0(t) - \sum_{i=1}^{\mathcal{N}-1} I_i\mathcal{V}_i(t)\right) = \frac{1}{I_{\mathcal{N}}}\left(\eta_4(t) - I_0\eta_3(t) - \sum_{i=1}^{\mathcal{N}-1} I_i\mathcal{V}_i(t)\right).
\end{aligned} \tag{2.23}$$

Based on the information included in this subsection and the recent one, we obtain the following compact form

$$\begin{aligned}
\dot{\mathcal{U}}_n(t) &= -\sum_{i=1}^{\mathcal{N}-1}\lambda_{n,i}\mathcal{V}_i(t) - \lambda_{n,0}\eta_3(t) - \frac{\lambda_{n,\mathcal{N}}}{I_{\mathcal{N}}}\left(\eta_4(t) - I_0\eta_3(t) - \sum_{i=1}^{\mathcal{N}-1} I_i\mathcal{V}_i(t)\right)\\
&- \gamma(\mathcal{U}_n^2(t) + \mathcal{V}_n^2(t))\left(\rho_{n,0}\eta_1 + \frac{\rho_{n,\mathcal{U}}}{I_{\mathcal{N}}}\left(\eta_2(t) - I_0\eta_1(t) - \sum_{i=1}^{\mathcal{N}-1} I_i\mathcal{U}_i(t)\right) + \sum_{i=1}^{\mathcal{N}-1}\rho_{n,i}\mathcal{U}_i(t)\right),\\
\dot{\mathcal{V}}_n(t) &= \sum_{i=1}^{\mathcal{N}-1}\lambda_{n,i}\mathcal{U}_i(t) + \lambda_{n,0}\eta_1(t) + \frac{\lambda_{n,\mathcal{N}}}{I_{\mathcal{N}}}\left(\eta_2(t) - I_0\eta_1(t) - \sum_{i=1}^{\mathcal{N}-1} I_i\mathcal{U}_i(t)\right)\\
&- \gamma(\mathcal{U}_n^2(t) + \mathcal{V}_n^2(t))\left(\rho_{n,0}\eta_3 + \frac{\rho_{n,\mathcal{U}}}{I_{\mathcal{N}}}\left(\eta_4(t) - I_0\eta_3(t) - \sum_{i=1}^{\mathcal{N}-1} I_i\mathcal{V}_i(t)\right) + \sum_{i=1}^{\mathcal{N}-1}\rho_{n,i}\mathcal{V}_i(t)\right),
\end{aligned} \tag{2.24}$$

subject to the initial values

$$\mathcal{U}_n(0) = f_1(x_{\mathcal{L},\mathcal{N},n}^{(\alpha_1,\beta_1)}), \quad \mathcal{V}_n(0) = f_2(x_{\mathcal{L},\mathcal{N},n}^{(\alpha_1,\beta_1)}), \quad n = 1,\ldots,\mathcal{N}-1, \tag{2.25}$$

this provide temporal differential system with initial conditions. The numerical approach of such system will listed in Subsection 2.3.

2.3. System of Temporal Differential Equations

Here, we numerically treat the temporal differential system with initial conditions

$$\begin{gathered}
\dot{\mathcal{W}}_r(t) = \mathcal{G}_r(t, \mathcal{W}_1(t), \cdots, \mathcal{W}_{\mathcal{R}}(t)), \quad 0 < \alpha < 1, \quad r = 1,\ldots,\mathcal{R}, \quad t \in [0, T],\\
\mathcal{W}_r(0) = \tau_r, \quad r = 1,\ldots,\mathcal{R},
\end{gathered} \tag{2.26}$$

where, $\mathcal{G}_r(t, \mathcal{W}_1(t),\ldots,\mathcal{W}_{\mathcal{R}}(t)), \quad r = 1,\ldots,\mathcal{R}$, are given functions. Shifted Jacobi–Gauss–Radau collocation is assigned for temporal discretization, which is more reliable for treating with such problems. We approximate $\mathcal{W}_r(t)$ as

$$\mathcal{W}_r(t) = \sum_{j=0}^{\mathcal{M}} a_{r,j}\mathcal{P}_{T,j}^{(\alpha_2,\beta_2)}(t), \quad r = 1,\ldots,\mathcal{R}. \tag{2.27}$$

The temporal derivative $\dot{\mathcal{W}}_r(t)$ is evaluated as

$$\dot{\mathcal{W}}_r(t) = \sum_{j=0}^{\mathcal{M}} a_{r,j}\frac{j + \alpha_2 + \beta_2 + 1}{T}\mathcal{P}_{T,j-1}^{(\alpha_2+1,\beta_2+1)}(t), \quad r = 1,\ldots,\mathcal{R}. \tag{2.28}$$

Thus, we get

$$\begin{gathered}
\Omega_r(t) = \sum_{j=0}^{\mathcal{M}} a_{r,j}\frac{j + \alpha_2 + \beta_2 + 1}{T}\mathcal{P}_{T,j-1}^{(\alpha_2+1,\beta_2+1)}(t) - \mathcal{G}_r\left(t, \sum_{j=0}^{\mathcal{M}} a_{1,j}\mathcal{P}_{T,j}^{(\alpha_2,\beta_2)}(t),\ldots,\sum_{j=0}^{\mathcal{M}} a_{\mathcal{K},j}\mathcal{P}_{T,j}^{(\alpha_2,\beta_2)}(t)\right) = 0,\\
r = 1,\ldots,\mathcal{R}, \quad t \in [0, T],
\end{gathered} \tag{2.29}$$

and

$$\sum_{j=0}^{\mathcal{M}} a_{r,j}\mathcal{P}_{T,j}^{(\alpha_2,\beta_2)}(0) = \tau_r, \quad r = 1,\ldots,\mathcal{R}. \tag{2.30}$$

Combining the initial conditions with the above-mentioned equations and equalizing the residual of (2.26) by zero at $(\mathcal{R}\mathcal{H})$ shifted Jacobi–Gauss–Radau collocation points give us

$$\Omega_r(t_{T,\mathcal{H},s}^{(\alpha_2,\beta_2)}) = 0, \quad r = 1,\ldots,\mathcal{R}, \quad s = 1,\ldots,\mathcal{H}, \tag{2.31}$$

the rest $(\mathcal{R})$ algebraic equations are outputted by the initial conditions as

$$\sum_{j=0}^{\mathcal{M}} a_{r,j}\mathcal{P}_{T,j}^{(\alpha_2,\beta_2)}(0) = \tau_r, \quad r = 1,\ldots,\mathcal{R}. \tag{2.32}$$

Finally, we have $(\mathcal{R}(\mathcal{H}+1))$ algebraic equations

$$\begin{gathered}\Omega_r(t_{T,\mathcal{H},s}^{(\alpha_2,\beta_2)}) = 0, \quad r = 1,\ldots,\mathcal{R}, \quad s = 1,\ldots,\mathcal{H},\\ \sum_{j=0}^{M} a_{r,j}\mathcal{P}_{T,j}^{(\alpha_2,\beta_2)}(0) = \tau_r, \quad r = 1,\ldots,\mathcal{R}.\end{gathered} \tag{2.33}$$

The numerical approach of the previous system will acquired by using Newton's iterative method.

3. APPLICATIONS AND NUMERICAL RESULTS

Here, the adequacy of the spectral collocation algorithms is verified by the obtained results. Problems including local and nonlocal conditions are examined. Mathematica version 10 is utilized to carry out the code.

Example 1. We test the next problem:

$$i\frac{\partial \mathcal{Z}}{\partial t} + \frac{\partial^2 \mathcal{Z}}{\partial x^2} + i\left|\mathcal{Z}\right|^2\frac{\partial \mathcal{Z}}{\partial t} = 0, \quad (x,t) \in [0,2\pi]\times[0,1], \tag{3.1}$$

the initial condition, the boundary conditions are given such as the continuous problem has the next exact solution

$$\mathcal{Z}(x,t) = e^{i(x-2t)}. \tag{3.2}$$

In Table 1, the numerical results based on the maximum absolute errors obtained using the previous algorithms are listed. Where

$$\begin{gathered}E_{\mathcal{U}_{\mathcal{N},\mathcal{M}}}(x,t) = \left|\mathcal{U}_{\mathcal{N},\mathcal{M}}(x,t) - \mathcal{U}(x,t)\right|, \quad (x,t) \in [0,\mathcal{L},T],\\ E_{\mathcal{V}_{\mathcal{N},\mathcal{M}}}(x,t) = \left|\mathcal{V}_{\mathcal{N},\mathcal{M}}(x,t) - \mathcal{V}(x,t)\right|, \quad (x,t) \in [0,\mathcal{L},T],\\ E_{\mathcal{N},\mathcal{M}}(x,t) = \sqrt{(E_{\mathcal{U}_{\mathcal{N},\mathcal{M}}}(x,t))^2 + (E_{\mathcal{V}_{\mathcal{N},\mathcal{M}}}(x,t))^2}, \quad (x,t) \in [0,\mathcal{L},T],\end{gathered}$$

and

$$\begin{gathered}M_{\mathcal{U}_{\mathcal{N},\mathcal{M}}}(x,t) = Max\{E_{\mathcal{U}_{\mathcal{N},\mathcal{M}}}(x,t)\ \forall (x,t) \in [0,\mathcal{L},T]\},\\ M_{\mathcal{V}_{\mathcal{N},\mathcal{M}}}(x,t) = Max\{E_{\mathcal{V}_{\mathcal{N},\mathcal{M}}}(x,t)\ \forall (x,t) \in [0,\mathcal{L},T]\},\\ M_{\mathcal{N},\mathcal{M}}(x,t) = Max\{E_{\mathcal{N},\mathcal{M}}(x,t)\ \forall (x,t) \in [0,\mathcal{L},T]\}.\end{gathered}$$

Space graphs of real and imaginary parts of the numerical solution of problem (3.1) are shown in Fig. 1, where $\alpha_1 = \beta_1 = \frac{1}{2}$, $\alpha_2 = \beta_2 = -\frac{1}{2}$, $\mathcal{N} = \mathcal{M} = 22$. While in Fig. 2, we recognize the outright matching of numerical and exact solutions in its real and imaginary parts, where $\alpha_1 = \beta_1 = \frac{1}{2}$, $\alpha_2 = \beta_2 = 0$, $\mathcal{N} = \mathcal{M} = 22$. Also, t-directions curves for real and imaginary parts are plotted in Fig. 3, where $\alpha_1 = \beta_1 = \alpha_2 = \beta_2 = 0$, $\mathcal{N} = \mathcal{M} = 22$. Moreover, we sketched in Fig. 4 the logarithmic graphs of $M_{\mathcal{E}}$ (i.e., $\log_{10} M_{\mathcal{E}}$) obtained by the present method with different values of $(\mathcal{N} = \mathcal{M} = 2,4,6,\ldots,22)$ for the given two cases.

Table 1. Maximum absolute errors of problem (3.1)

$(\mathcal{N},\mathcal{M})$	$M_{\mathcal{U}_{\mathcal{N},\mathcal{M}}}$	$M_{\mathcal{V}_{\mathcal{N},\mathcal{M}}}$	$M_{\mathcal{N},\mathcal{M}}$	$M_{\mathcal{U}_{\mathcal{N},\mathcal{M}}}$	$M_{\mathcal{V}_{\mathcal{N},\mathcal{M}}}$	$M_{\mathcal{N},\mathcal{M}}$
	$\alpha_1=\beta_1=\frac{1}{2},\ \alpha_2=\beta_2=-\frac{1}{2}$			$\alpha_1=\beta_1=\alpha_2=\beta_2=\frac{1}{2}$		
(2,2)	3	2.43947	3	3	2.45368	3
(6,6)	1.40114×10^{-1}	8.58788×10^{-2}	1.40114×10^{-1}	1.40114×10^{-1}	9.91275×10^{-2}	1.40114×10^{-1}
(10,10)	2.69366×10^{-4}	1.55293×10^{-4}	2.69366×10^{-4}	2.69366×10^{-4}	1.5104×10^{-4}	2.69366×10^{-4}
(14,14)	1.76464×10^{-7}	1.73355×10^{-7}	1.78742×10^{-7}	9.3633×10^{-8}	7.02974×10^{-8}	9.3633×10^{-8}
(18,18)	2.8662×10^{-11}	2.01341×10^{-11}	2.96815×10^{-11}	9.86863×10^{-12}	7.24454×10^{-12}	9.86863×10^{-12}
(22,22)	3.38618×10^{-15}	2.10942×10^{-15}	3.57703×10^{-15}	4.60743×10^{-15}	4.21885×10^{-15}	4.82021×10^{-15}
	$\alpha_1=\beta_1=\alpha_2=\beta_2=0$			$\alpha_1=\alpha_2=\frac{1}{2},\ \beta_1=\beta_2=0$		
(2,2)	2	1.54616	2	2.31443	2.19137	2.35555
(6,6)	7.65346×10^{-2}	5.90733×10^{-2}	7.65346×10^{-2}	8.9755×10^{-2}	7.52669×10^{-2}	9.14316×10^{-2}
(10,10)	1.26474×10^{-4}	8.50239×10^{-5}	1.26474×10^{-4}	1.87895×10^{-4}	1.72272×10^{-4}	1.98787×10^{-4}
(14,14)	3.89901×10^{-8}	3.843×10^{-8}	3.89901×10^{-8}	3.06267×10^{-7}	4.22171×10^{-7}	4.34246×10^{-7}
(18,18)	3.72602×10^{-12}	2.83817×10^{-12}	3.72602×10^{-12}	1.08205×10^{-11}	1.10754×10^{-11}	1.17568×10^{-11}
(22,22)	2.9976×10^{-15}	3.88578×10^{-15}	3.92523×10^{-15}	5.44009×10^{-15}	6.43929×10^{-15}	8.42966×10^{-15}

Example 2. Now, consider the following

$$i\frac{\partial\mathscr{Z}}{\partial t}+\frac{\partial^2\mathscr{Z}}{\partial x^2}+i|\mathscr{Z}|^2\frac{\partial\mathscr{Z}}{\partial t}=0,\quad (x,t)\in[0,1]\times[0,1], \tag{3.3}$$

with the initial, boundary and integral conditions

$$\mathscr{Z}(0,t)=e^{-2it},\quad \int_0^1\mathscr{Z}(x,t)dx=-i(-1+e^{i})e^{-2it},\quad \mathscr{Z}(x,0)=e^{ix}, \tag{3.4}$$

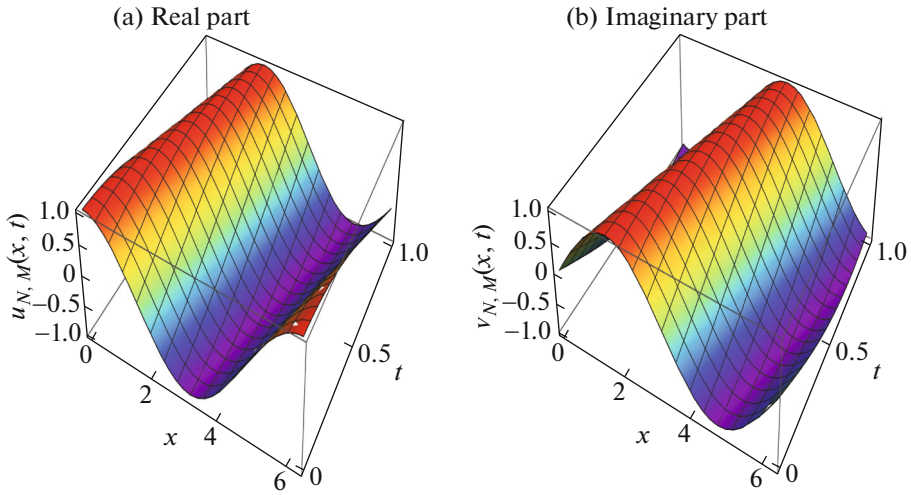

Fig. 1. Space graphs of real and imaginary parts of the numerical solution of problem (3.1).

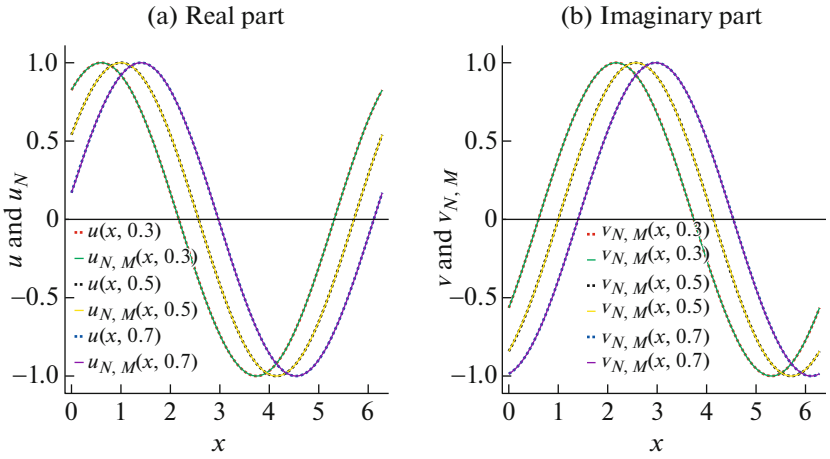

Fig. 2. x-directions curves for the approximate and exact solutions of real and imaginary parts of problem (3.1).

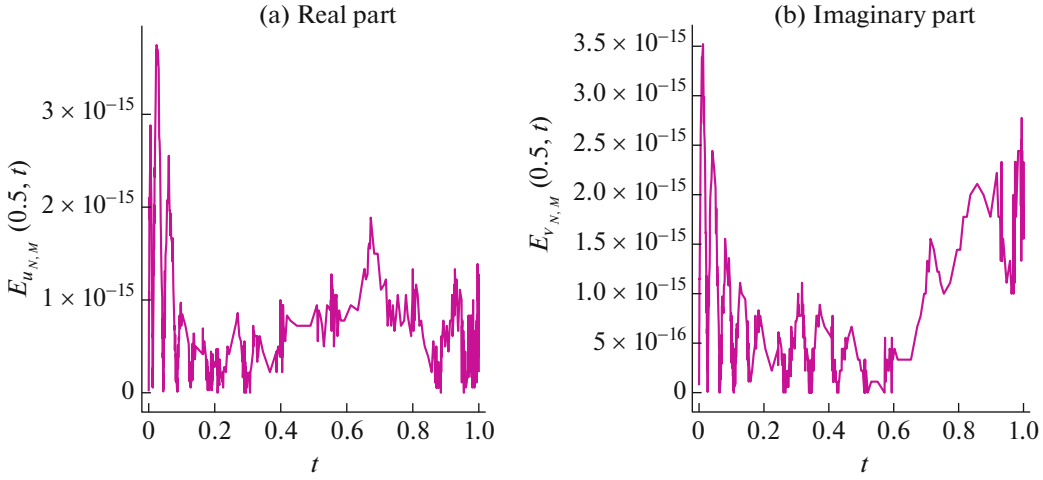

Fig. 3. t-directions curves of real and imaginary parts of the absolute error of problem (3.1).

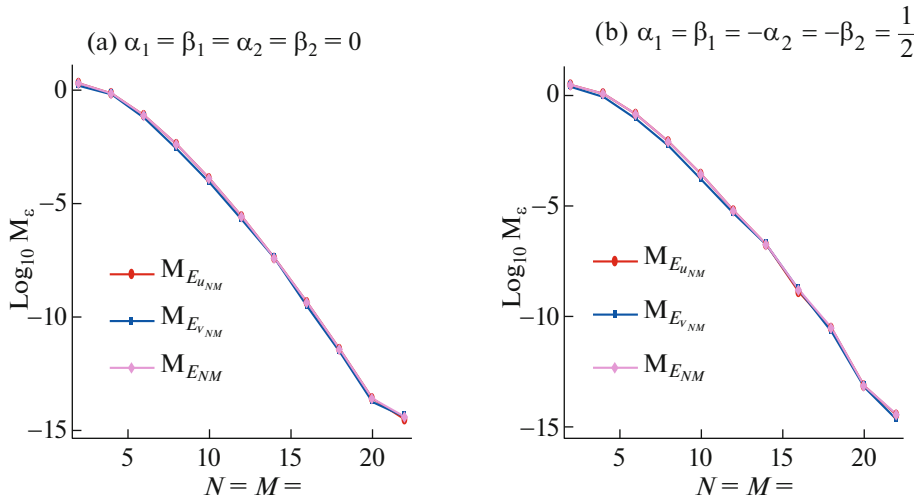

Fig. 4. $M_{\mathscr{E}}$ convergence of problem (3.1).

Table 2. Maximum absolute errors of problem (3.3)

$(\mathcal{N},\mathcal{M})$	$M_{\mathcal{U}_{\mathcal{N},\mathcal{M}}}$	$M_{\mathcal{V}_{\mathcal{N},\mathcal{M}}}$	$M_{\mathcal{N},\mathcal{M}}$	$M_{\mathcal{U}_{\mathcal{N},\mathcal{M}}}$	$M_{\mathcal{V}_{\mathcal{N},\mathcal{M}}}$	$M_{\mathcal{N},\mathcal{M}}$
	$\alpha_1 = \beta_1 = \alpha_2 = \beta_2 = 0$			$\alpha_1 = \beta_1 = \frac{1}{2}, \alpha_2 = \beta_2 = 0$		
(2,2)	3.28221×10^{-1}	6.81393×10^{-1}	7.56323×10^{-1}	2.18004×10^{-1}	4.73801×10^{-1}	5.21549×10^{-1}
(4,4)	1.678×10^{-2}	4.09803×10^{-2}	4.42827×10^{-2}	9.65256×10^{-3}	2.98926×10^{-2}	3.14125×10^{-2}
(8,8)	1.53505×10^{-6}	3.61387×10^{-6}	3.92637×10^{-6}	8.57355×10^{-7}	2.50059×10^{-6}	2.64348×10^{-6}
(12,12)	2.01904×10^{-11}	3.31546×10^{-11}	3.88185×10^{-11}	1.38719×10^{-11}	2.2471×10^{-11}	2.64079×10^{-11}
(16,16)	1.09024×10^{-13}	6.23113×10^{-14}	1.15051×10^{-13}	6.34492×10^{-14}	8.70415×10^{-14}	9.24781×10^{-14}
	$\alpha_1 = 0, \beta_1 = -\alpha_2 = -\beta_2 = \frac{1}{2}$			$\alpha_1 = \alpha_2 = \frac{1}{2}, \beta_1 = \beta_2 = -\frac{1}{2}$		
(2,2)	1.25532×10^{-1}	3.93666×10^{-1}	4.04973×10^{-1}	1.15929×10^{-1}	2.85836×10^{-1}	3.08451×10^{-1}
(4,4)	5.47096×10^{-3}	1.80896×10^{-2}	1.84737×10^{-2}	2.9547×10^{-3}	1.55312×10^{-2}	1.57013×10^{-2}
(8,8)	6.91267×10^{-7}	1.15202×10^{-6}	1.34351×10^{-6}	5.57136×10^{-7}	9.12882×10^{-7}	1.06946×10^{-6}
(12,12)	7.68041×10^{-12}	1.04553×10^{-11}	1.29731×10^{-11}	6.43552×10^{-12}	8.31712×10^{-12}	1.05162×10^{-11}
(16,16)	1.24067×10^{-13}	8.09353×10^{-14}	1.24409×10^{-13}	1.13909×10^{-13}	1.99174×10^{-13}	1.99436×10^{-13}

the exact solution for the previous equation is

$$\mathcal{Y}(x,t) = e^{i(x-2t)}. \tag{3.5}$$

In Table 2, the numerical results based on the maximum absolute errors obtained using the previous algorithms are listed. Space graphs of real and imaginary parts of the absolute error of problem (3.3) are shown in Fig. 5, where $\alpha_1 = \beta_1 = \alpha_2 = \beta_2 = 0$, $\mathcal{N} = \mathcal{M} = 16$. While in Figs. 6–8, x- and t-directions curves for absolute errors $E_{\mathcal{U}_{\mathcal{N},\mathcal{M}}}$, $E_{\mathcal{V}_{\mathcal{N},\mathcal{M}}}$, $E_{\mathcal{N},\mathcal{M}}$ are plotted, where $\alpha_1 = \beta_1 = \alpha_2 = \beta_2 = 0$, $\mathcal{N} = \mathcal{M} = 16$. Even though few values of N and M, the accurate results have been spotted in these tables. This is consistent with which was predicted in case of using a spectral collocation method. Likewise, these results bring to light the reasonability convergence of the shifted Jacobi collocation method for such problems.

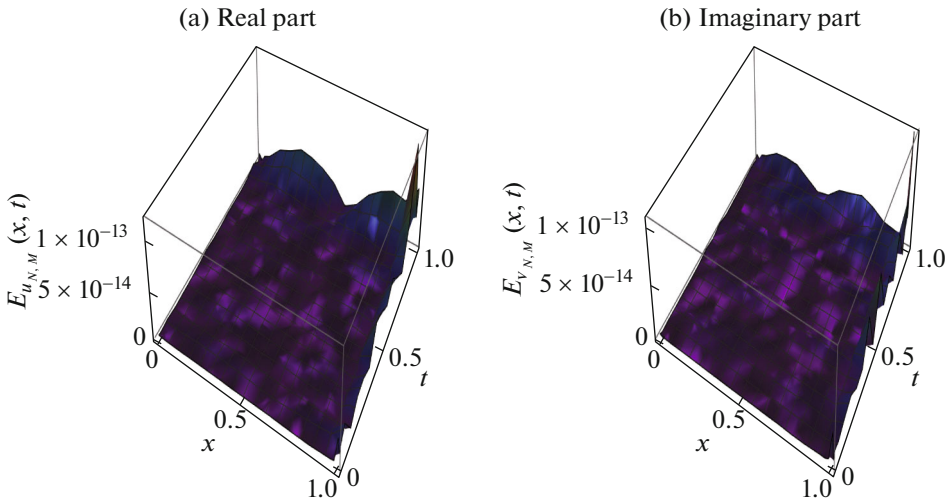

Fig. 5. Space graphs of real and imaginary parts of the absolute error of problem (3.3).

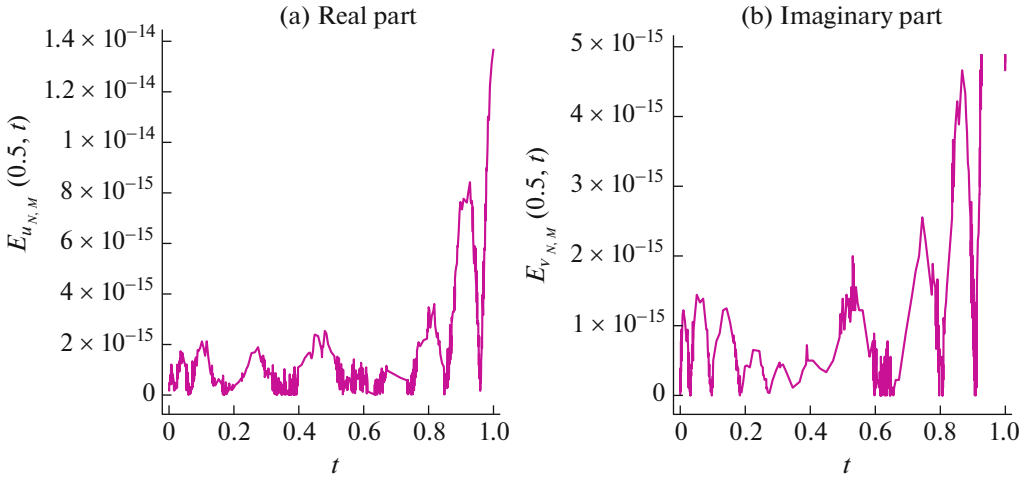

Fig. 6. t-graphs of real and imaginary parts of the absolute error of problem (3.1).

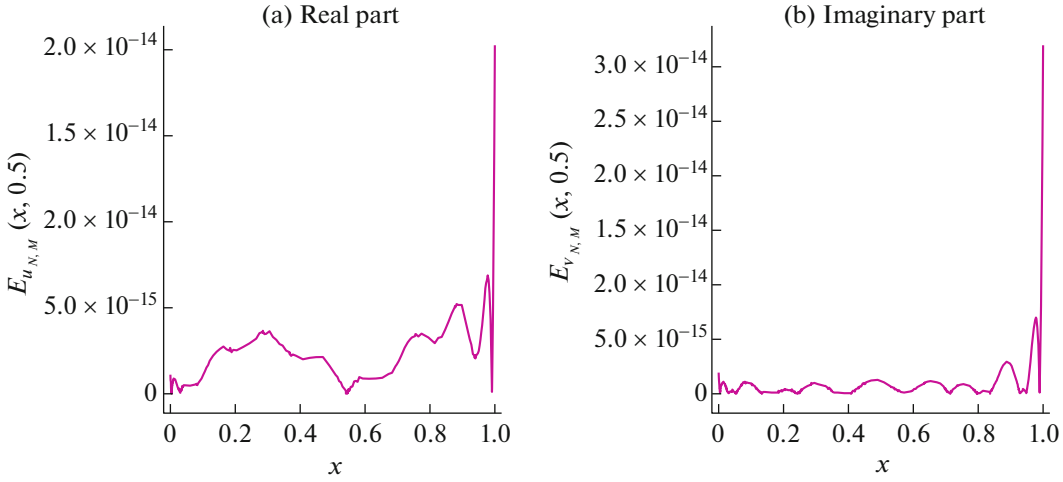

Fig. 7. x-graphs of real and imaginary parts of the absolute error of problem (3.1).

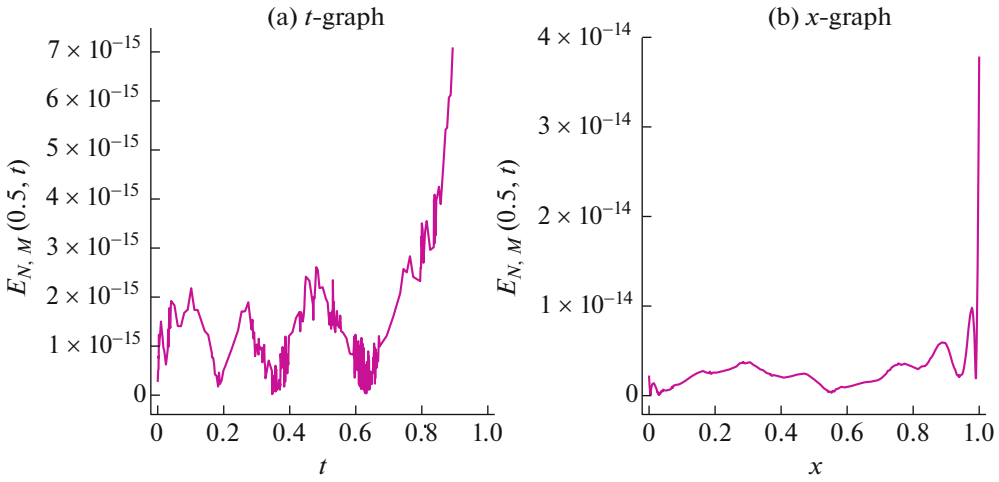

Fig. 8. t-graphs of real and imaginary parts of the absolute error of problem (3.1).

4. CONCLUSIONS

This paper adopted fully shifted Jacobi's collocation method to study Chen–Lee–Liu equation that discusses soliton propagation down the optical fibers with perturbation terms incorporated into the waveguides. The powerful numerical scheme gave way to a number of impressive numerical results that prove high efficiency of the algorithm. The study was carried out with both local and nonlocal conditions.

The results of the algorithm pave way to conduct further additional research in this field to display additional results in future. One avenue is to consider Chen–Lee–Liu equation with differential group delay and then further along study the model with additional optoelectronic devices such as in magneto-optic waveguides. Subsequently, this model will be treated with the same algorithm for DWDM topology. Thus, a lot lies in the bucket list!

REFERENCES

1. A.-M. Wazwaz and L. Kaur, "Optical solitons and Peregrine solitons for nonlinear Schrödinger equation by the variational iteration method," Optik **179**, 804–809 (2019).
2. H. Triki and A.-M. Wazwaz, "Combined optical solitary waves of the Fokas–Lennels equation," Waves Random Complex Media **27** (4), 587–593 (2017).
3. A.-M. Wazwaz and L. Kaur, "Complex simplified Hirota's forms and Lie symmetry analysis for multiple real and complex soliton solutions of the modified KdV–sine-Gordon equation," Nonlinear Dyn. **95** (3), 2209–2215 (2019).
4. A.-M. Wazwaz, "Two-mode fifth-order KdV equations: Necessary conditions for multiple-soliton solutions to exist," Nonlinear Dyn. **87** (3), 1685–1691 (2017).
5. A.-M. Wazwaz, "Multiple soliton solutions and multiple complex soliton solutions for two distinct Boussinesq equations," Nonlinear Dyn. **85** (2), 731–737 (2016).
6. E. H. Doha, A. H. Bhrawy, M. A. Abdelkawy, and R. A. Van Gorder, "Jacobi–Gauss–Lobatto collocation method for the numerical solution of 1+1 nonlinear Schrödinger equations," J. Comput. Phys. **261**, 244–255 (2014).
7. H. Wang, "Numerical studies on the split step finite difference method for the nonlinear Schrödinger equations," Appl. Math. Comput. **170**, 17–35 (2005).
8. M. Dehghan and A. Taleei, "Numerical solution of nonlinear Schrödinger equation by using time-space pseudo-spectral method," Numer. Methods Partial Differ. Equations **26**, 979–992 (2010).
9. M. Dehghan and A. Taleei, "A Chebyshev pseudo-spectral multi-domain method for the soliton solution of coupled nonlinear Schrödinger equations," Comput. Phys. Commun. **182**, 2519–2529 (2011).
10. L. Kaur and A.-M. Wazwaz, "Bright-dark optical solitons for Schrödinger–Hirota equation with variable coefficients," Optik **179**, 479–484 (2019).
11. H. H. Chen, Y. C. Lee, and C. S. Liu, "Integrability of nonlinear Hamiltonian systems by inverse scattering method," Phys. Scr. **20**, 490–492 (1979).
12. E. G. Fan, "Integrable systems of derivative nonlinear Schrödinger type and their multi-Hamiltonian structure," J. Phys. A: Math. Gen. **34**, 513–519 (2001).
13. J. Zhang, W. Liu, D. Qiu, Y. Zhang, K. Porsezian, and J. He, "Rogue wave solutions of a higher-order Chen–Lee–Liu equation," Phys. Scr. **90**, 055207 (2015).
14. A. J. M. Jawad, A. Biswas, Q. Zhou, M. Alfiras, S. P. Moshokoa, and M. Belic, "Chirped singular and combo optical solitons for Chen–Lee–Liu equation with three forms of integration architecture," Optik—Int. J. Light Electron Opt. Optics **178**, 172–177 (2019).
15. A. Biswas, M. Ekici, A. Sonmezoglu, A. S. Alshomrani, Q. Zhou, S. P. Moshokoa, and M. Belic, "Chirped optical solitons of Chen–Lee–Liu equation by extended trial equation scheme," Optik **156**, 999–1006 (2018).
16. Y. Yildirim, "Optical solitons to Chen–Lee–Liu model with modified simple equation approach," Optik—Int. J. Light Electron Opt. **183**, 792–796 (2019).
17. Y. Yildirim, "Optical solitons to Chen–Lee–Liu model in birefringent fibers with trial equation approach," Optik—Int. J. Light Electron Opt. **183**, 881–886 (2019).
18. H. Triki, Y. Hamaizi, Q. Zhou, A. Biswas, M. Z. Ullah, S. P. Moshokoa, and M. Belic, "Chirped singular solitons for Chen–Lee–Liu equation in optical fibers and PCF," Optik **157**, 156–160 (2018).
19. A. Biswas, "Chirp-free bright optical soliton perturbation with Chen–Lee–Liu equation by traveling wave hypothesis and semi-inverse variational principle," Optik—Int. J. Light Electron Opt. **172**, 772–776 (2018).
20. A. S. H. F. Mohammed, H. O. Bakodah, M. A. Banaja, A. A. Alshaery, Q. Zhou, A. Biswas, S. P. Moshokoa, and M. R. Belic, "Bright optical solitons of Chen–Lee–Liu equation with improved Adomian decomposition method," Optik—Int. J. Light Electron Opt. **181**, 964–970 (2019).
21. B. Yang, W.-G. Zhang, H.-Q. Zhang, and S.-B. Pei, "Generalized Darboux transformation and rational soliton solutions for Chen–Lee–Liu equation," Appl. Math. Comput. **242**, 863–876 (2014).

22. F. S. Sousa, C. F. Lages, J. L. Ansoni, A. Castelo, and A. Simao, "A finite difference method with meshless interpolation for incompressible flows in non-graded tree-based grids," J. Comput. Phys. **396**, 848–866 (2019).
23. N. A. Mbroh and J. B. Munyakazi, "A fitted operator finite difference method of lines for singularly perturbed parabolic convection–diffusion problems," Math. Comput. Simul. **165**, 156–171 (2019).
24. H. M. Patil and R. Maniyeri, "Finite difference method based analysis of bio-heat transfer in human breast cyst," Thermal Sci. Eng. Prog. **10**, 42–47 (2019).
25. P.-W. Li, Z.-J. Fu, Y. Gu, and L. Song, "The generalized finite difference method for the inverse Cauchy problem in two-dimensional isotropic linear elasticity," Int. J. Solids Struct. **174–175**, 69–84 (2019).
26. S. Ray, S. B. Degweker, and U. Kannan, "A hybrid method for reactor core simulations employing finite difference and polynomial expansion with improved treatment of transverse leakage," Ann. Nuclear Energy **131**, 102–111 (2019).
27. Y. Shu, J. Li, and C. Zhang, "A local and parallel Uzawa finite element method for the generalized Navier–Stokes equations," Appl. Math. Comput. **387**, 124671 (2020).
28. C. Wang and J. Wang, "Primal-dual weak Galerkin finite element methods for elliptic Cauchy problems," Comput. Math. Appl. **79** (3), 746–763 (2020).
29. E. Burman, P. Hansbo, M. G. Larson, A. Massing, and S. Zahedi, "A stabilized cut streamline diffusion finite element method for convection–diffusion problems on surfaces," Comput. Methods Appl. Mech. Eng. **358** (2020). arXiv:1807.01480.
30. X. Xiao, Z. Dai, and X. Feng, "A positivity preserving characteristic finite element method for solving the transport and convection–diffusion–reaction equations on general surfaces," Comput. Phys. Commun. **247** (3), 106941 (2020).
31. E. H. Doha, A. H. Bhrawy, and S. S. Ezz-Eldien, "A Chebyshev spectral method based on operational matrix for initial and boundary value problems of fractional order," Comput. Math. Appl. **62** (5), 2364–2373 (2011).
32. E. H. Doha, M. A. Abdelkawy, A. Z. M. Amin, and A. M. Lopes, "Shifted Jacobi–Gauss–collocation with convergence analysis for fractional integro-differential equations," Commun. Nonlinear Sci. Numer. Simul. **72**, 342–359 (2019).
33. E. H. Doha, M. A. Abdelkawy, A. Z. M. Amin, and D. Baleanu, "Shifted Jacobi spectral collocation method with convergence analysis for solving integro-differential equations and system of integro-differential equations," Nonlinear Anal.: Model. Control **24** (3), 332–352 (2019).
34. A. H. Bhrawy, T. M. Taha, and J. A. Tenreiro Machado, "A review of operational matrices and spectral techniques for fractional calculus," Nonlinear Dyn. **81** (3), 1023–105 (2015).
35. M. A. Zaky, I. G. Ameen, and M. A. Abdelkawy, "A new operational matrix based on Jacobi wavelets for a class of variable-order fractional differential equations," Proc. Rom. Acad. Ser. A **18** (4), 315–322 (2017).
36. A. H. Bhrawy and M. A. Zaky, "A method based on the Jacobi tau approximation for solving multi-term time-space fractional partial differential equations," J. Comput. Phys. **281**, 876–895 (2015).
37. E. H. Doha, A. H. Bhrawy, D. Baleanu, and R. M. Hafez, "A new Jacobi rational-Gauss collocation method for numerical solution of generalized pantograph equations," Appl. Numer. Math. **77**, 43–54 (2014).
38. V. Kolmanovskii and A. Myshkis, *Applied Theory of Functional Differential Equations* (Kluwer Academic, Amsterdam, 1992).
39. A. H. Bhrawy and M. A. Abdelkawy, "Fully spectral collocation approximation for multi-dimensional fractional Schrödinger equations," J. Comput. Phys. **294**, 462–483 (2015).
40. A. H. Bhrawy, E. H. Doha, D. Baleanu, and S. S. Ezz-eldein, "A spectral tau algorithm based on Jacobi operational matrix for numerical solution of time fractional diffusion-wave equations," J. Comput. Phys. **293**, 142–156 (2015).
41. E. H. Doha, R. M. Hafez, and Y. H. Youssri, "Shifted Jacobi spectral-Galerkin method for solving hyperbolic partial differential equations," Comput. Math. Appl. **78** (3), 889–904 (2019).
42. E. H. Doha and W. M. Abd-Elhameed, "Efficient spectral ultraspherical-dual-Petrov–Galerkin algorithms for the direct solution of (2n+1)th-order linear differential equations," Math. Comput. Simul. **79** (11), 3221–3242 (2009).
43. H. Triki, M. M. Babatin, and A. Biswas, "Chirped bright solitons for Chen–Lee–Liu equation in optical fibers and PCF," Optik **149**, 300–303 (2017).
44. H. Triki, Q. Zhou, S. P. Moshokoa, M. Z. Ullah, A. Biswas, and M. Belic, "Chirped W-shaped optical solitons of Chen–Lee–Liu equation," Optik **55**, 208–212 (2018).
45. H. Triki, Y. Hamaizi, Q. Zhou, A. Biswas, M. Z. Ullah, S. P. Moshokoa, and M. Belic, "Chirped dark and gray optical solitons for Chen–Lee–Liu equation in optical fibers and PCF," Optik **155**, 329–333 (2018).
46. A. H. Kara, A. Biswas, Q. Zhou, L. Moraru, S. P. Moshokoa, and M. Belic, "Conservation laws for optical solitons with Chen–Lee–Liu equation," Optik **174**, 195–198 (2018).
47. O. Gonzalez-Gaxiola and A. Biswas, "W-shaped optical solitons of Chen–Lee–Liu equation by Laplace–Adomian decomposition method," Opt. Quantum Electron. **50** (8), 1–11 (2020).